Diffusion approximation and short-path statistics at low to intermediate Knudsen numbers

Guillaume Terrée, Stephane Blanco, Mouna El-Hafi, Richard Fournier, Julien Yves Rolland

Diffusion approximation and short-path statistics at low to intermediate Knudsen numbers

Guillaume Terrée[1], Stéphane Blanco[2,3], Mouna El Hafi[1], Richard Fournier[2,3] and Julien Yves Rolland[4]

[1] *Université de Toulouse; Centre RAPSODEE, UMR CNRS 5302, Mines Albi; Campus Jarlard F-81013 Albi Cedex 09, France*
[2] *Université de Toulouse, UPS, INPT; LAPLACE (Laboratoire Plasma et Conversion d'Energie) 118 route de Narbonne, F-31062 Toulouse cedex 9, France*
[3] *CNRS, LAPLACE - F-31062 Toulouse cedex 9, France*
[4] *LMB, UMR CNRS 6623, Université de Franche-Comté - 16, route de Gray, 25030 Besançon Cedex, France*

Abstract – In the field of first-return statistics in bounded domains, short paths may be defined as those paths for which the diffusion approximation is inappropriate. However, general integral constraints have been identified that make it possible to address such short-path statistics indirectly by application of the diffusion approximation to long paths in a simple associated first-passage problem. This approach is exact in the zero Knudsen limit (Blanco S. and Fournier R., *Phys. Rev. Lett.*, **97** (2006) 230604). Its generalization to the low to intermediate Knudsen range is addressed here theoretically and the corresponding predictions are compared to both one-dimension analytical solutions and three-dimension numerical experiments. Direct quantitative relations to the solution of the Schwarzschild-Milne problem are identified.

A simple invariance property of diffusion random walks was independently identified in [1] and [2]: for particles incident on a system Ω, distributed uniformly and isotropically at its boundary, the average length $\langle L \rangle$ of the particle trajectories inside the system before the first exit is invariant when changing the characteristics of the random walk (exponentially distributed path lengths and micro-reversibly distributed scattering directions); highly or weakly scattering, and isotropic, forward or backward scattering particles lead to the same average trajectory length, that is therefore only dependent on the system geometry. For three-dimension walks

$$\langle L \rangle = \frac{4V}{S}, \tag{1}$$

where V is the volume of Ω and S the surface of its boundary $\partial\Omega$. Numerous applications were reported in fields such as biology, colloid physics, turbid media and radiative transfer [3–13]. Theoretical extensions were also addressed by Benichou and co-workers [14], providing significant advances in our understanding of random search strategies [15–17] and contributing to the field of Brownian motion in confined geometries [18–20] (see also [21] for a review). A very significant and recent step forward was also made in [22], where the property could be rigorously extended to the scattering of waves in resonant, chaotic or Anderson-localized structures. Major advances can also be expected from the numerous contributions of Mazzolo and co-workers that have closely considered the links between the physics and mathematics literatures, in particular with the introduction of this property in the field of integral geometry as a generalization of the Cauchy formula [23–27], and a reconciliation with the Feynman-Kac formalism [28–31]. Their researches, especially those addressing the full length distribution [32], led to the identification of the following second property [33]: for any function f of the trajectory length, with a defined limit f_0 in zero,

$$\langle f(L) \rangle = f_0 + \langle L \rangle \langle f'(R) \rangle, \tag{2}$$

where R is the random variable corresponding to trajectory lengths until the first exit for particles starting uniformly and isotropically from within the volume, with the only constraint that $\lim_{x \to +\infty} p_R(x) f(x) = 0$, where p_R is

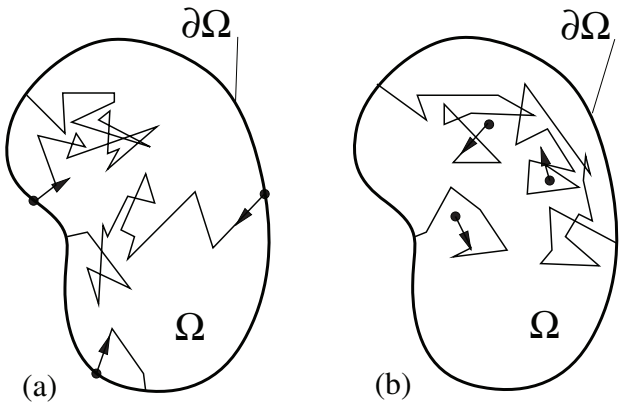

Fig. 1: Illustration of first-return L trajectories (a) and first-passage R trajectories (b).

the probability density function of R (see fig. 1(b)). The main interest of eq. (2) may be summarized the following way [33]: L trajectories start at the boundary and therefore always include a non-negligible amount of short paths (particle returning to the boundary after a few scattering events, see fig. 1(a)) for which the diffusion approximation is inappropriate. In this sense, evaluating $\langle f(L)\rangle$ is a first-return problem. But $\langle f(L)\rangle$ can be exactly related to $\langle L\rangle$ and $\langle f'(R)\rangle$, where $\langle L\rangle$ is a known geometric quantity (see eq. (1)), and $\langle f'(R)\rangle$ is the solution of a first-passage problem, which is easier to handle (in the present context) using the diffusion approximation because the contribution of short paths decreases with the Knudsen number. We may therefore write $\langle f(L)\rangle$ in the zero Knudsen limit as

$$\langle f(L)\rangle|_{Kn\to 0} = f_0 + \langle L\rangle\langle f'(R_{\text{diff}})\rangle, \tag{3}$$

where R_{diff} is the random variable corresponding to the diffusion approximation applied to R.

The particular case in which $f(x) = x^n$, with n a strictly positive integer value, corresponds to the evaluation of the positive moments of L. The limit f_0 is null and eq. (3) becomes

$$\langle L^n\rangle|_{Kn\to 0} = \langle L\rangle n\langle R_{\text{diff}}^{n-1}\rangle. \tag{4}$$

According to the properties of macroscopic diffusion, R_{diff} scales as $k = 1/\lambda^*$, where λ^* is the transport mean free path (λ^* reduces to the mean free path in the particular case of isotropic diffusion). This leads to

$$\langle L^n\rangle|_{Kn\to 0} = \alpha_n k^{n-1}, \tag{5}$$

where α_n is only dependent on the system geometry, and not on the random walk characteristics. This result was pointed out in [33,34] as highlighting the contribution of short paths to $\langle L^n\rangle$: if only long L trajectories were to contribute to $\langle L^n\rangle$, the diffusion approximation could be directly applied on L and $\langle L^n\rangle$ would scale as k^n instead of k^{n-1}. The authors then proposed a detailed physical picture for this quite counterintuitive reduction of the exponent of k by 1 due to short-path statistics. Essentially, large path-lengths scale indeed as k^n but the probability to enter deep enough in the system scales as $1/k$.

Coming back to the general case, eq. (3) is directly relevant to numerous application problems in which the numerical evaluation of first-return statistics in real geometries is either unfeasible or incompatible with computation time requirements. Such simulations use either stochastic methods of the Monte Carlo type, or deterministic methods based on phase-space discretisation of transport equations. Both approaches are known as computationally very demanding and the alternative consisting in the evaluation of $\langle f'(R_{\text{diff}})\rangle$ using any standard numerical solution of the macroscopic diffusion equation is obviously orders of magnitude faster, and is tractable whatever the geometrical complexity. One such practical example is optical diagnostic, in which numerical treatments are required for inversion of the measured signals, with real-time constraints (in particular in the pharmaceutic and medical domains) which are such that solving the macroscopic diffusion equation is about the maximum affordable computational cost [35]. But what about all practical configurations in which intermediate Knudsen levels are encountered? We know that eq. (1) is rigorously valid independently of the Knudsen level: is there more behind this property that could be used for the evaluation of $\langle f(L)\rangle$ outside the zero Knudsen limit? In particular, can we obtain some theoretical benefits of the above-mentioned physical picture explaining why $\langle L^n\rangle|_{Kn\to 0}$ scales as k^{n-1}? These questions are addressed hereafter according to the following sequence: Available analytical solutions in the one-dimensional case are used to explore how eq. (5) is modified when increasing the Knudsen value. The observed features lead us to the proposition of an approximate polynomial form of $\langle L^n\rangle$ in the general case. We then address the question of practically evaluating the polynomial coefficients for complex three-dimensional geometries, highlighting quantitative relations to the solution of the Schwarzschild-Milne problem [36,37].

The characteristics of a diffusion random walk are entirely known given the mean free path $\lambda(\boldsymbol{x})$ (the average of the exponentially distributed path lengths between successive scattering events) and the single scattering phase function $p(\boldsymbol{u}_s; \boldsymbol{u}_i, \boldsymbol{x})$ (the probability density function of the scattering direction $\boldsymbol{u}_s$ for an incident direction $\boldsymbol{u}_i$). Both are functions of the location $\boldsymbol{x}$. When considering one-dimension walks (displacement along a line with instantaneous direction changes), the phase function can be chosen arbitrarily. Here we make the choice of isotropic scattering, which means that at each scattering event the probabilities to turn backward and to keep the same direction are both 1/2. In the particular case in which the mean free path is uniform and the considered system Ω is a segment of length a, the following analytical solution is available for $\langle L^n\rangle$ [33]:

$$\langle (L/a)^n\rangle_{1\text{D}} = \sum_{i=0}^{n-1} \beta_{i,n} \frac{1}{Kn^i} \tag{6}$$

Table 1: $\beta_{i,n}$ coefficients of the polynomial approximations of $\langle L^n \rangle$ (see eq. (7)), for the one-dimentionnal walk described in the text, as well as for three-dimensional walks in five geometries: a slab, a cube, a sphere, a spherical shell enclosed by two concentric spheres of radius R and $2R$, and a volume composed of three identical cubes assembled according to a L shape (called *tricube*). For each geometry, a has been chosen equal to $\langle L \rangle$: $\langle L \rangle$ is indeed equal to the segment length in the one-dimensional case; and $\langle L \rangle$ is computed with eq. (1) for the three-dimensional geometries. The "line" coefficients are all analytical. For the five other configurations: $\beta_{0,1}$ is obtained with eq. (1); $\beta_{n-1,n}$ are obtained as proposed in [33]; $\beta_{n-2,n}$ are computed with eq. (14); the other coefficients are evaluated, knowing $\beta_{n-1,n}$ and $\beta_{n-2,n}$, using MC simulations. The MC simulations evaluate both $\langle L^n \rangle$ and $\partial \langle L^n \rangle / \partial Kn$ between $1/Kn = 10$ and $1/Kn = 50$, and the displayed corresponding $\beta_{i,n}$ coefficients are the result of a Gauss-Markov linear fit (read [38]); for thus evaluated coefficients, an estimation of the calculus error is given in square brackets. The number of sampled trajectories is about 10^9.

	Line	Slab	Sphere	Spherical shell	Cube	Tricube
$\beta_{0,1}$	1	1	1	1	1	1
$\beta_{1,2}$	$1/6$	0.125	0.225	0.1394	0.2724	0.2531
$\beta_{0,2}$	1	1.066	1.066	1.115	1.288	1.295
$\beta_{2,3}$	$1/20$	28.13e-3	0.1085	35.80e-3	0.1707	0.1433
$\beta_{1,3}$	$1/2$	0.3996	0.7193	0.4751	1.131	1.068
$\beta_{0,3}$	1	1.828 [0.009]	1.235 [0.007]	2.050 [0.007]	2.187 [0.003]	2.357 [0.005]
$\beta_{3,4}$	$17/840$	8.538e-3	73.23e-3	12.46e-3	0.1526	0.1155
$\beta_{2,4}$	$17/60$	0.1698	0.6243	0.2314	1.300	1.132
$\beta_{1,4}$	$11/10$	1.292 [0.004]	1.764 [0.005]	1.626 [0.006]	3.959 [0.008]	3.992 [0.007]
$\beta_{0,4}$	1	4.564 [0.075]	1.794 [0.022]	5.857 [0.081]	3.214 [0.027]	4.214 [0.028]

with $Kn = \lambda/a$. The constants $\beta_{i,n}$ are given in table 1 (in the "Line" column) up to $n = 4$. The n-th moment of L is therefore a polynomial function of degree $n-1$ of the inverse of the Knudsen number. At the zero Knudsen limit, only the monome of higher degree remains and $\langle (L/a)^n \rangle_{1\mathrm{D}} \mid_{Kn \to 0} = \beta_{n-1,n}/Kn^{n-1}$, which is compatible with the theoretical predictions of [33], with $\alpha_n = \beta_{n-1,n} a^{2n-1}$ (see eq. (5)).

With this simple academic example, we can explore the accuracy level corresponding to the straightforward application of eq. (5) outside the zero Knudsen limit. The conclusions are that the 1% accuracy level is only reached beyond $1/Kn = 590$ for $\langle L^2 \rangle$, $1/Kn = 980$ for $\langle L^3 \rangle$ and $1/Kn = 1390$ for $\langle L^4 \rangle$. Even a 10% accuracy level requires that the Knudsen number remains below $1/Kn = 50$ (see the first line of table 2). Other calculations made on three-dimensional geometries lead to similar conclusions (see "monome" in table 2). This strongly restrains the range of the possible practical use of the theoretical derivations of [33], in particular for medical applications where the accuracy requirements are high and the Knudsen numbers always greater than 10^{-2}.

But the fact that the exact solution of the 1D problem has a polynomial shape over the whole Knudsen range gives us a simple indication concerning a possible extension of eq. (5) to the intermediate Knudsen range for any dimension and any geometry. Outside the one-dimensional case, eq. (6) can indeed be seen as a polynomial approximation of $\langle L^n \rangle$ in the limit $Kn \to 0$:

$$\langle (L/a)^n \rangle = \sum_{i=0}^{n-1} \beta_{i,n} \frac{1}{Kn^i} + O(Kn) \qquad (7)$$

with $Kn = 1/(ka)$ and a any length scale characteristic of the considered system geometry. The meaning of such a polynomial approximation is directly related to the fact that eq. (5) leads to $\lim_{Kn \to 0} Kn^{n-1} \langle (L/a)^n \rangle = \frac{\alpha_n}{a^{2n-1}}$ and the coefficients $\beta_{i,n}$ are the n first coefficients of the Taylor expansion of $Kn^{n-1} \langle (L/a)^n \rangle$ with respect to Kn around $Kn = 0$. We held numerical experiments to explore the validity of eq. (7) in the low to intermediate Knudsen range. The coefficients $\beta_{i,n}$, obtained by model fitting of Monte Carlo simulations, are given in table 1. The relative accuracies of resulting $\langle L^n \rangle$ predictions are better when decreasing the Knudsen range, as was observed with the monomial model of [33], but they are now of a few percent, or below one percent, in the Knudsen range typical of the above-listed applications (see the lines "polynome" in table 2).

For this modeling approach to become fully practical, the remaining question is: how to make the $\beta_{i,n}$ coefficients easily accessible to those who want to estimate the moments of L in any new geometry? A first solution is to perform Monte Carlo simulations, fit them with eq. (7), and mount tables of $\beta_{i,n}$ coefficients for different geometry classes. Such computations are very demanding, but they are to be done only once, as the $\beta_{i,n}$ are purely geometric quantities.

We also started to think of pure theoretical alternatives. In [33], an exact expression was provided for the first coefficient ($\beta_{n-1,n}$) as the solution of a macroscopic diffusion process. The idea was that $\langle L^n \rangle = \langle L \rangle \, n \, \langle R^{n-1} \rangle$ could be expressed in an integral manner using the first-passage time probability density function (that of the R configuration, *i.e.* when particles start uniformly within the volume), and that this density was the solution of a macroscopic diffusion problem with null density at the boundary. Using a Hilbertian approach (expanding the distribution function), it can be shown that this solution corresponds

Table 2: Lower bound values of $1/Kn$ which with a 1% or 10% accuracy can be reached using the monomial [33], binomial, and polynomial approximations. The "line", "slab", "sphere", "spherical shell", "cube", and "tricube" configurations are described in the caption of table 1.

Precision	1%			10%		
Moment	$\langle L^2\rangle$	$\langle L^3\rangle$	$\langle L^4\rangle$	$\langle L^2\rangle$	$\langle L^3\rangle$	$\langle L^4\rangle$
line, monome	594	988	1390	54	88.0	130
line, binome	0	39.8	66.2	0	9.32	15.6
line, polynome	0	0	0	0	0	0
slab, monome	840	1400	2000	77	130	190
slab, binome	24	74	110	4.1	19	30
slab, polynome	24	16	12	4.1	4.3	4.1
sphere, monome	470	660	850	43	61	79
sphere, binome	3.4	31	45	0	7.5	12
sphere, polynome	3.4	3.9	1.2	0	0	0
spherical shell, monome	790	1300	1800	72	120	170
spherical shell, binome	22	69	110	0	17	28
spherical shell, polynome	22	12	6.3	0	0.69	2.9
cube, monome	470	660	850	43	62	80
cube, binome	6.7	32	47	0	7.9	12
cube, polynome	6.7	2.9	0	0	0	0
tricube, monome	510	740	970	46	69	92
tricube, binome	8.4	37	54	0	8.9	14
tricube, polynome	8.4	2.5	0.62	0	0	0

to a first-order approximation in Knudsen number. But the same Hilbertian reasoning establishes that the approximation becomes accurate to second order when using the *Milne boundary condition* [39]. This implies that both $\beta_{n-1,n}$ and $\beta_{n-2,n}$ can be deduced from the diffusion approximation as

$$\begin{aligned}\tfrac{a^n}{n\langle L\rangle}\,\beta_{n-1,n} &= \lim_{Kn\to 0}\big(Kn^{n-1}\langle R^{n-1}\rangle\big)\\ &= \lim_{Kn\to 0}\big(Kn^{n-1}\langle R^{n-1}_{\rm diff}\rangle\big),\end{aligned} \tag{8}$$

$$\begin{aligned}\tfrac{a^n}{n\,\langle L\rangle}\,\beta_{n-2,n} &= \lim_{Kn\to 0}\tfrac{\partial}{\partial Kn}\big(Kn^{n-1}\langle R^{n-1}\rangle\big)\\ &= \lim_{Kn\to 0}\tfrac{\partial}{\partial Kn}\big(Kn^{n-1}\langle R^{n-1}_{\rm diff}\rangle\big),\end{aligned} \tag{9}$$

where $Kn^{n-1}\langle R^{n-1}_{\rm diff}\rangle$ reads

$$Kn^{n-1}\langle R^{n-1}_{\rm diff}\rangle = \Big(\frac{q}{a}\Big)^{n-1}\int_0^{+\infty} p_{\rm diff}(\tau)\tau^{n-1}{\rm d}\tau, \tag{10}$$

with q the problem dimension and $p_{\rm diff}$ the probability density of the dimensionless first-passage time at the macroscopic diffusion limit, using Milne boundary conditions. This density writes

$$p_{\rm diff}(\tau) = \int_{\partial\Omega} \boldsymbol{u}\cdot\boldsymbol{\nabla}\rho(\boldsymbol{x};\tau,Kn){\rm d}\boldsymbol{x}, \tag{11}$$

$$\begin{aligned}&\partial_\tau\rho(\boldsymbol{x};\tau,Kn)=\boldsymbol{\nabla}^2\rho(\boldsymbol{x};\tau,Kn), && \forall(\boldsymbol{x};\tau)\in\Omega\times[0;+\infty[,\\ &\rho(\boldsymbol{x};\tau,Kn)=\Lambda a Kn\,\boldsymbol{u}\cdot\boldsymbol{\nabla}\rho(\boldsymbol{x};\tau,Kn),\\ &\quad\forall(\boldsymbol{x};\tau)\in\partial\Omega\times]0;+\infty[,\\ &\rho(\boldsymbol{x};0,Kn)=1/V, && \forall\boldsymbol{x}\in\Omega,\end{aligned} \tag{12}$$

where $\boldsymbol{u}$ is the inward normal unit vector at the boundary and Λ the extrapolation length. $\Lambda = 1$ in the one-dimentional case, and $\Lambda \simeq 0.710446$ in three dimensions with isotropic scattering [40]. Consequently, $\beta_{n-1,n}$ and $\beta_{n-2,n}$ are directly related to the solutions, at $Kn = 0$, of both the diffusion problem of eq. (12) and its associated derived one in $s = \frac{1}{\Lambda a}\frac{\partial\rho}{\partial Kn}$. This leads to the following coupled macroscopic diffusion problem:

$$\begin{cases}\partial_\tau\rho(\boldsymbol{x};\tau,0) = \boldsymbol{\nabla}^2\rho(\boldsymbol{x};\tau,0), & \forall(\boldsymbol{x};\tau)\in\Omega\times[0;+\infty[,\\ \partial_\tau s(\boldsymbol{x};\tau,0) = \boldsymbol{\nabla}^2 s(\boldsymbol{x};\tau,0), & \\ \rho(\boldsymbol{x};\tau,0) = 0, & \\ s(\boldsymbol{x};\tau,0) = \boldsymbol{u}\cdot\boldsymbol{\nabla}\rho(\boldsymbol{x};\tau,0), & \forall(\boldsymbol{x};\tau)\in\partial\Omega\times]0;+\infty[,\\ \rho(\boldsymbol{x};0,0) = 1/V, & \\ s(\boldsymbol{x};0,0) = 0, & \forall\boldsymbol{x}\in\Omega,\end{cases} \tag{13}$$

the solution of which allows to address $\beta_{n-1,n}$ as in [33] and $\beta_{n-2,n}$ as

$$\begin{aligned}\beta_{n-2,n} &= \Lambda\,\frac{\langle L\rangle\, n\, q^{n-1}}{a^{2n-2}}\int_0^{+\infty} p_{{\rm diff},s}(\tau)\tau^{n-1}{\rm d}\tau,\\ p_{{\rm diff},s}(\tau) &= \textstyle\int_{\partial\Omega}\boldsymbol{u}\cdot\boldsymbol{\nabla}s(\boldsymbol{x};\tau,0)\cdot{\rm d}\boldsymbol{x}.\end{aligned} \tag{14}$$

These expressions are exact, which explains why $\beta_{n-1,n}$ and $\beta_{n-2,n}$ have no associated uncertainty values in table 1 where they are provided for a slab, a sphere, a cube, a tricube, and a spherical shell. Monte Carlo simulations were only used for $\beta_{i,n}$ with $i \leqslant n-3$. In practice, if Monte Carlo simulations cannot be afforded, then these last coefficients can be neglected as a first modeling approach. The binomial results of table 2 illustrate that this is sufficient to extend by one order of magnitude the range of Knudsen numbers addressed in [33].

REFERENCES

[1] Bardsley J. N. and Dubi A., *SIAM J. Appl. Math.*, **40** (1981) 71.
[2] Blanco S. and Fournier R., *Europhys. Lett.*, **61** (2003) 168.
[3] Eymet V., Fournier R., Dufresne J.-L., Lebonnois S., Hourdin F. and Bullock M. A., *J. Geophys. Res.*, **114** (2009) E11008.
[4] Anikeenko A. V., Medvedev N. N., Kovalev M. K. and Melgunov M. S., *J. Geophys. Res.*, **50** (2009) 403.
[5] Levitz P., *J. Phys.: Condens. Matter*, **17** (2005) S4059.
[6] Challet M., Fourcassie V., Blanco S., Fournier R., Theraulaz G. and Jost C., *Naturwissenschaften*, **92** (2005) 367.
[7] Eymet V., Fournier R., Blanco S. and Dufresne J.-L., *J. Quant. Spectrosc. Radiat. Transfer*, **91** (2005) 27.
[8] Jeanson R., Blanco S., Fournier R., Deneubourg J.-L., Fourcassié V. and Theraulaz G., *J. Theor. Biol.*, **225** (2003) 443.
[9] Benichou O., Loverdo C., Moreau M. and Voituriez R., *J. Chem. Soc.*, **10** (2008) 7059.
[10] Condamin S., Tejedor V., Voituriez R., Benichou O. and Klafter J., *Proc. Natl. Acad. Sci. U.S.A.*, **105** (2008) 5675.
[11] Vitkin E., Turzhitsky V., Qui L., Guo L. Y., Itzkan I., Hanlon E. B. and Perelman L. T., *Nature (London)*, **2** (2011) 587.
[12] Weitz S., Blanco S., Fournier R., Gautrais J., Jost C. and Theraulaz G., *Phys. Rev. E*, **89** (2014) 52715.
[13] Zoia A., Dumonteil E. and Mazzolo A., *Phys. Rev. E*, **84** (2011) 61130.
[14] Bénichou O., Coppey M., Moreau M., Suet P. H. and Voituriez R., *Europhys. Lett.*, **70** (2005) 42.
[15] Tejedor V., Voituriez R. and Benichou O., *Phys. Rev. Lett.*, **108** (2012) 88103.
[16] Benichou O., Loverdo C., Moreau M. and Voituriez R., *Rev. Mod. Phys.*, **83** (2011) 81.
[17] Bénichou O., Loverdo C., Moreau M. and Voituriez R., *J. Phys.: Condens. Matter*, **19** (2007) 065141.
[18] Condamin S., Bénichou O. and Moreau M., *Phys. Rev. E*, **75** (2007) 021111.
[19] Grebenkov D. S., *Phys. Rev. E*, **76** (2007) 41139.
[20] Chevalier C., Bénichou O., Meyer B. and Voituriez R., *J. Phys. A*, **44** (2011) 025002.
[21] Bénichou O. and Voituriez R., *Phys. Rep.*, **539** (2014) 225.
[22] Pierrat R., Ambichl P., Gigan S., Haber A., Carminati R. and Rotter S., *Proc. Natl. Acad. Sci. U.S.A.*, **111** (2014) 17765.
[23] Mazzolo A., Roesslinger B. and Gille W., *J. Math. Phys. (N.Y.)*, **44** (2003) 6195.
[24] Mazzolo A., *J. Phys. A*, **37** (2004) 7095.
[25] Mazzolo A., Mulatier C. and Zoia A., *J. Math. Phys.*, **55** (2014) 83308.
[26] Mazzolo A., *J. Phys. A*, **42** (2009) 105002.
[27] Mazzolo A., *Ann. Nucl. Sci. Eng.*, **35** (2008) 503.
[28] Zoia A., Dumonteil E. and Mazzolo A., *EPL*, **100** (2012) 40002.
[29] Zoia A., Dumonteil E. and Mazzolo A., *Phys. Rev. E*, **85** (2012) 11132.
[30] Zoia A., Dumonteil E. and Mazzolo A., *Phys. Rev. E*, **84** (2011) 21139.
[31] Zoia A., Dumonteil E. and Mazzolo A., *Phys. Rev. Lett.*, **106** (2011) 220602.
[32] Mazzolo A., *Europhys. Lett.*, **68** (2004) 350.
[33] Blanco S. and Fournier R., *Phys. Rev. Lett.*, **97** (2006) 230604.
[34] Rolland J., PhD Thesis (Toulouse) 2009.
[35] Jacques L. and Pogue B. W., *J. Biomed. Opt.*, **13** (2008) 041302.
[36] Chandrasekhar S., *Radiative Transfer* (Dover Publications) 1960.
[37] Ishimaru A., *Wave Propagation and Scattering in Random Media* (IEEE Press) 1977.
[38] Orlande H. R. B., Fudym O., Maillet D. and Cotta R. M., *Thermal Measurements and Inverse Techniques* (CRC Press) 2011.
[39] Degond P. and Mas-Gallic S., *Transp. Theor. Stat. Phys.*, **16** (1987) 589.
[40] Weinberg A. M. and Wigner E. P., *The Physical Theory of Neutron Chain Reactors* (Chigago Press) 1958.